Heliyon 10 (2024) e38507

Contents lists available at ScienceDirect

Heliyon

journal homepage: www.cell.com/heliyon

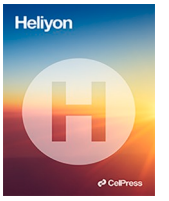

Research article

Succinic semialdehyde derived from the gut microbiota can promote the proliferation of adult T-cell leukemia/lymphoma cells

Nodoka Chiba [a], Shinya Suzuki [a], Daniel Enriquez-Vera [c], Atae Utsunomiya [d], Yoko Kubuki [e], Tomonori Hidaka [e], Kazuya Shimoda [e], Shingo Nakahata [b,c,*,1], Takuji Yamada [a,g,h,i,**,1], Kazuhiro Morishita [b,f,***,1]

[a] *School of Life Science and Technology, Tokyo Institute of Technology, Meguro, Tokyo, Japan*
[b] *Division of Tumor and Cellular Biochemistry, Department of Medical Sciences, University of Miyazaki, Kiyotake, Miyazaki, Japan*
[c] *Division of HTLV-1/ATL Carcinogenesis and Therapeutics, Joint Research Center for Human Retrovirus Infection, Kagoshima University, Sakuragaoka, Kagoshima, Japan*
[d] *Department of Hematology, Imamura General Hospital, Kamoikeshinmachi, Kagoshima, Japan*
[e] *Division of Hematology, Diabetes, and Endocrinology, Department of Internal Medicine, Faculty of Medicine, University of Miyazaki, Kiyotake, Miyazaki, Japan*
[f] *Project for Advanced Medical Research and Development, Project Research Division, Frontier Science Research Center, University of Miyazaki, Kiyotake, Miyazaki, Japan*
[g] *Metagen, Inc., Yamagata, Japan*
[h] *Metagen Theurapeutics, Inc., Yamagata, Japan*
[i] *digzyme, Inc., Tokyo, Japan*

A B S T R A C T

Adult T-cell leukemia/lymphoma (ATLL) is a refractory blood cancer with severe immunodeficiency resulting from retroviral infection. ATLL develops in only 5 % of HTLV-1-infected individuals, but the entire mechanism of ATLL progression remains unknown. Since recent studies have reported that the gut microbiome influences the progression of various diseases, we hypothesized that ATLL is also related to the gut microbiome and aimed to investigate this relationship.

We analyzed the taxonomic and functional profiles of the gut microbiota of ATLL patients (n = 28) and HTLV-1-infected individuals (n = 37). We found that the succinic semialdehyde (SSA) synthesis pathway was significantly enriched in the gut microbiome of ATLL patients (P = 0.000682), and *Klebsiella*, whose abundance was significantly greater in ATLL patients and high-risk HTLV-1-infected individuals (P = 0.0326), was the main contributor to this pathway. Administration of SSAs to ATLL cell lines resulted in significant cell proliferation.

Herein, we propose that the gut microbiome can regulate ATLL progression via metabolites.

* Corresponding author. Division of Tumor and Cellular Biochemistry, Department of Medical Sciences, University of Miyazaki, Kiyotake, Miyazaki, Japan.

** Corresponding author. School of Life Science and Technology, Tokyo Institute of Technology, Meguro, Tokyo, Japan.

*** Corresponding author. Division of Tumor and Cellular Biochemistry, Department of Medical Sciences, University of Miyazaki, Kiyotake, Miyazaki, Japan.

E-mail addresses: snakahata@kufm.kagoshima-u.ac.jp (S. Nakahata), takuji@bio.titech.ac.jp (T. Yamada), kmorishi@med.miyazaki-u.ac.jp (K. Morishita).

[1] These authors contributed equally to this work.

https://doi.org/10.1016/j.heliyon.2024.e38507
Received 2 May 2024; Received in revised form 20 September 2024; Accepted 25 September 2024
Available online 2 October 2024

1. Introduction

Gut microbes produce various metabolites that influence gastrointestinal functions, including those influencing local and systemic immunity [1]. However, specific metabolites produced by the gut microbiota may have harmful effects [2] and the specific gut microbiota contributes to opportunistic infections [3]. Notably, a reduction in gut microbiota populations that release substances that activate gut barrier function and suppress immunity has been linked to leukemia development. For example, in acute myeloid leukemia (AML), the release of lipopolysaccharide (LPS) into the bloodstream, accompanied by a decrease in intestinal barrier function due to changes in the gut microbiome, may contribute to the deterioration of AML [4]. In addition, several other associations between hematologic tumors and the gut microbiome have been reported [5–7]. One specific type of leukemia is adult T-cell leukemia/lymphoma (ATLL), which is caused by the oncogenic retrovirus human T-cell leukemia virus type 1 (HTLV-1), and ATLL is an endemic virus that affects an estimated 5–10 million individuals worldwide [8]. HTLV-1 infects and transforms host T cells through the viral-encoded oncoprotein Tax over an extended period, followed by clonal expansion due to the presence of HTLV-1/HBZ and the accumulation of genomic and epigenomic abnormalities in HTLV-1-infected T cells, ultimately leading to leukemia-lymphoma. ATLL symptoms manifest as leukemic cell infiltration into organs and opportunistic infections, resulting in decreased survival rates [9]. While 95 % of HTLV-1-infected individuals remain asymptomatic throughout their lifetime and are called asymptomatic HTLV-1 carriers, approximately 5 % develop ATLL after decades of infection [10]. However, the specific factors contributing to ATLL initiation and progression have not been identified, suggesting the involvement of specific host factors.

Immunosuppressive states, such as those amenable to the development of opportunistic infections, may promote the development of ATLL [11]. In HTLV-1 carriers coinfected with *Strongyloides stercoralis*, which is known to cause opportunistic infection, type 2 helper T cells are suppressed [12,13], increasing the susceptibility of HTLV-1 carriers to ATLL. Several gut microbes are also responsible for opportunistic infections [14]. In addition, opportunistic infections such as *Clostridium difficile* infection have been observed in HIV-infected patients, a disease-causing virus analogous to HTLV-1 [15], suggesting that fluctuations in the gut microbiome may play a role in disease progression [16]. Moreover, since ATLL cells frequently infiltrate the gut mucosa [17], ATLL cells may interact with the gut microbiome, including metabolites. Thus, we hypothesized that the gut microbiome may play a role in the development and progression of ATLL.

To investigate the significance of the gut microbiome in the development and progression of ATLL, we characterized the gut microbiomes of asymptomatic HTLV-1 carriers and patients with ATLL. We identified significantly enriched metabolic pathways associated with ATLL progression in gut microbes through shotgun metagenomic data analysis. Additionally, we validated our findings using *in vitro* experiments. We revealed that metabolites that are likely enriched in the guts of patients with ATLL can promote ATLL cell proliferation. Based on these findings, we propose a mechanism involving metabolites derived from the gut microbiome in the progression of ATLL.

2. Results

2.1. Overview of gut microbial analysis in patients with ATLL and asymptomatic HTLV-1 carriers

In this study, we aimed to identify the gut microbiome and factors related to the development and progression of ATLL. We obtained fecal samples from two cohorts because fecal samples were collected from asymptomatic HTLV-1 carriers at home after the hospital visit using a preservation solution kit [18], while fresh fecal samples were collected from patients with ATLL at the same time as hospital admission. Therefore, one cohort included asymptomatic HTLV-1 carriers (n = 37) and patients with ATLL (n = 11), most of whom had less advanced disease-type, such as the smoldering type, and healthy controls (n = 20) (cohort 1, Table 1). In the asymptomatic HTLV-1 carrier group, there were eight asymptomatic HTLV-1 carriers with HTLV-1 proviral loads (PVLs) above 40 (per 1000 peripheral blood mononuclear cells (PBMCs)), and we considered that they have a high risk for developing ATLL (high-risk

Table 1
Characteristics of the subjects in cohort 1.

		ATLL	Asymptomatic HTLV-1 Carrier	Healthy control
Number of subjects		11	37	20
Disease type	Acute	2	–	
	Lymphoma	0	–	–
	Chronic	1	–	–
	Smoldering	8	–	–
	High-risk carrier	–	8	–
	Low-risk carrier	–	29	–
Age		67.4 ± 5.1	60.6 ± 10.4	58.6 ± 3.0
Sex (F/M)		4:7	28:9	0:20
PVL (/1000PBMC)		243.0 ± 274.6	60.6 ± 91.3	–
sIL-2Ra(U/mL)		2564.8 ± 4357.5	450.1 ± 146.3	–
Chemotherapy prior to blood sampling		1	1	–
Chemotherapy prior to stool sampling		1	1	0
Antibiotics prior to blood sampling		2	4	–
Antibiotics prior to stool sampling		2	4	4

carriers) because it has been reported that asymptomatic HTLV-1 carriers with a PVL greater than 4 % have an increased risk of developing ATLL in a previous study [19]. The other cohort included patients with advanced-stage ATLL (n = 17), such as acute type, and healthy controls (n = 8) (cohort 2, Table 2). Most patients with ATLL in this study had a history of antibiotic use within one week of fecal collection to treat opportunistic infections because a symptom of ATLL is immunodeficiency.

We analyzed the gut microbiomes of ATLL patients and asymptomatic HTLV-1 carriers in cohort 1. The results showed that the abundance of *Klebsiella* was increased in patients with ATLL and high-risk HTLV-1 carriers. In addition, metagenomic data from cohort 2 suggested that the homoprotocatechuate (HPC) degradation pathway was significantly enriched in the gut microbiome of ATLL patients. The end product of this degradation pathway is succinic semialdehyde (SSA). Thus, we tested the efficacy of ATLL cells by adding them to ATLL cell lines derived from patients with ATLL. Notably, in lymphocytes, specific concentrations of SSA promoted cell proliferation.

In conclusion, this study identified a candidate ATLL progressor in the gut via *in silico* analysis, and we confirmed its function via *in vitro* experimental validation (Fig. 1).

2.2. The community structure of the gut microbiota in patients with ATLL and asymptomatic HTLV-1 carriers

We examined the gut microbiome of patients with ATLL and asymptomatic HTLV-1 carriers in both groups. Using 16S rRNA gene amplicon sequence data from cohort 1, we first conducted a principal component analysis (PCA) to compare the genus-level profiles. There were three ATLL subtypes in cohort 1: acute (n = 2), chronic (n = 1), and smoldering (n = 8). Several criteria define these subtypes and reflect ATLL progression and the risk of ATLL development [20].

The PCA results showed variability in the composition of the gut microbiota among the subjects, and the top four principal components were related to *Bacteroides* and *Prevotella* (Fig. 2A). These bacteria are known to contribute to enterotype [21]. The median relative abundance of the four bacterial genera characterizing each cluster was approximately 10 % (Fig. 2B). Fig. 2C shows the 30 genera with the highest average abundance. The Chao1 index, which represents the taxonomic alpha diversity, was significantly greater in patients with ATLL than in asymptomatic carriers (P = 0.0141) (Fig. 2D). The results obtained from cohort 2, which consisted of only patients with ATLL and healthy controls and no asymptomatic HTLV-1 carriers (Table 2), are shown in Supplementary Fig. S3.

Furthermore, to investigate which factors contribute to characterizing the gut microbiome of subjects, we performed a permutational multivariate analysis of variance (PERMANOVA) with Bray–Curtis distance (Supplementary Table 1). There were no significant differences between patients treated with antibiotics or chemotherapy and nonusers in cohort 1 (P > 0.05), although the gut microbial composition significantly differed among patients with different ATLL subtypes.

2.3. The specific gut microbial abundances differed between patients with ATLL and asymptomatic HTLV-1 carriers

To investigate individual bacterial abundance changes, we compared the abundances of each gut microbial genus in cohort 1 using 16S rRNA gene amplicon sequences. There were eight high-risk HTLV-1 carriers and 29 low-risk HTLV-1 carriers in the HTLV-1 asymptomatic carrier group in cohort 1.

Using the Kruskal–Wallis test, we identified 32 bacterial genera with differential abundance among the four groups (P < 0.05) (Fig. 3A, right column, “KW”). Further pairwise comparisons with the Brunner–Munzel test were also conducted between the two groups: patients with ATLL and high-risk HTLV-1 carriers (A + HiC) and healthy controls and low-risk HTLV-1 carriers (H + C). This comparison revealed 17 bacterial genera that exhibited significant differences in abundance between the two groups (P < 0.05) (Fig. 3A, left column, “BM”). Specifically, seven genera were significantly more abundant in the A + HiC group (Fig. 3A, left column, Fig. 3B), namely, *Eubacterium_R* (P = 0.0121); an unassigned bacterial genus from the Ruminococcaceae family labeled “Unassigned 40” (P = 0.0178); *Alistipes_A* (P = 0.0312); *Klebsiella* (P = 0.0326); *Desulfovibrio* (P = 0.0335); *Eubacterium_G* (P = 0.0343); and an unassigned bacterial genus from the Acidaminococcaceae family labeled “Unassigned 577” (P = 0.0419) (Fig. 3C). The results of the Kruskal–Wallis test for these seven bacteria are shown in Supplementary Fig. S4A. In addition, the distributions of these seven bacteria

Table 2
Characteristics of the subjects.

		ATLL	Asymptomatic HTLV-1 Carrier	Healthy control
Number of subjects		17	0	8
Disease type	Acute	12	–	–
	Lymphoma	5	–	–
	Chronic	0	–	–
	Smoldering	0	–	–
Age		68.5 ± 6.5	–	43.2 ± 9.4
Sex (F/M)		8:9	–	4:4
PVL (/1000PBMC)		478.9 ± 499.1	–	–
sIL-2Ra(U/mL)		16284.7 ± 13830.5	–	–
Chemotherapy prior to blood sampling		14	–	0
Chemotherapy prior to stool sampling		14	–	0
Antibiotics prior to blood sampling		16	–	0
Antibiotics prior to stool sampling		16	–	0

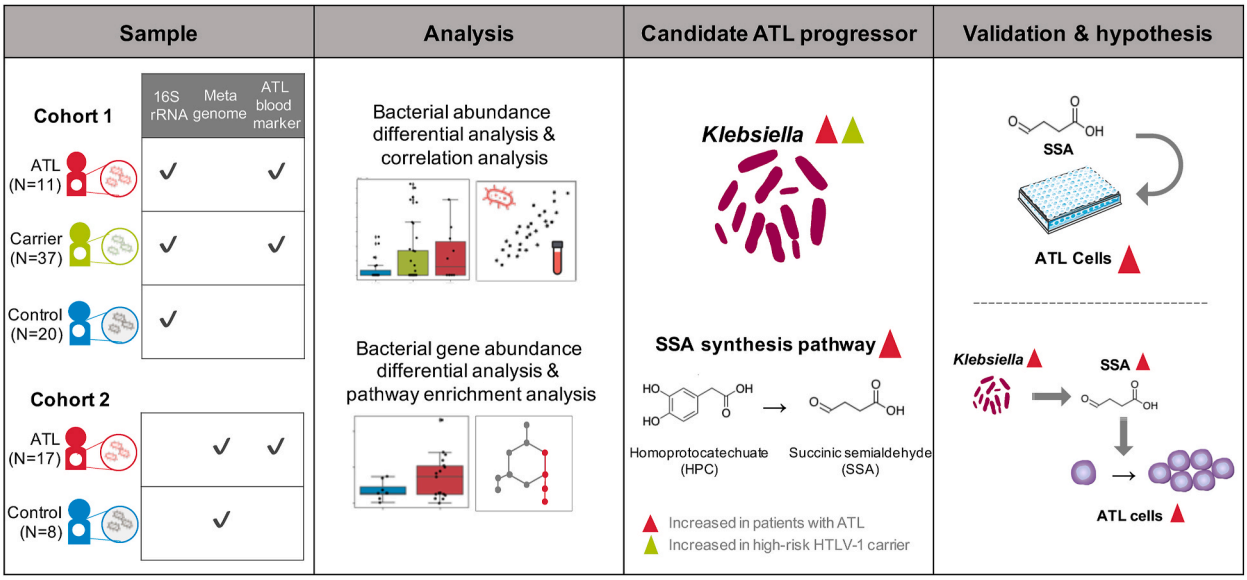

Fig. 1. Overview of this study.

in cohort 2 are shown in Supplementary Fig. S4B.

As a definitive result, we observe clear differences in the relative abundance of specific bacterial genera among ATLL patients, high-risk and low-risk HTLV-1 carriers, and healthy controls.

2.4. *The abundances of Klebsiella and Eubacterium_G were positively correlated with the ATLL-specific tumor markers*

To understand the relationships between the seven significantly increased gut microbial genera and the development and progression of ATLL, we investigated the correlation between the abundance of the increased gut microbial genera and soluble interleukin 2 receptor-alpha (sIL-2Ra) protein concentration, an ATLL biomarker that reflects ATLL progression, in the peripheral blood [22]. We analyzed gut microbial taxonomic profiles determined via 16S rRNA gene amplified sequences in both cohorts.

For high-risk HTLV-1 carriers and patients with ATLL in cohort 1, we did not find a positive correlation between sIL-2Ra levels and the two microbial abundances (*Eubacterium_G*: $\rho = -0.383$, *Klebsiella*: $\rho = 0.2$) (Fig. 4A–C). However, there were positive correlations between sIL-2Ra levels and these two microbial abundances in patients with ATLL in cohort 2 ($\rho = 0.733, 0.539$; Fig. 4B–D). The abundance of *Klebsiella* was significantly greater in the patients with ATLL than in the controls in both cohorts ($P = 0.0326, 0.0167$; Fig. 3C; Fig. 4F). In comparison, the abundance of *Eubacterium_G* was not significantly greater in cohort 2 ($P = 0.34$; Fig. 4F). The correlation analysis results for the other five candidate microbiota and sIL-2Ra levels are presented in Supplementary Fig. S5.

Furthermore, specific gut microbial abundances, such as those of *Coprococcus_B* and *Ruminococcus_E,* exhibited strong correlations with HTLV-1 proviral load values and sIL-2Ra levels (Supplementary Figs. S6 and S7).

Thus, several gut microbial abundances were correlated with ATLL biomarkers, and the abundances of *Eubacterium_G* and *Klebsiella* could be positively related to the progression of ATLL.

2.5. *The succinic semialdehyde synthesis pathway is enriched in the gut microbiome of patients with ATLL, promoting the proliferation of ATLL cells*

To explore the functional composition of the gut microbiota in patients with ATLL and the functions of the identified ATLL-associated candidate microbiota, we analyzed functional ortholog gene profiles from whole-genome shotgun sequencing data of fecal samples from patients with ATLL in cohort 2.

Through differential analysis of functional gene (KO) profiles, we identified 788 KOs with significantly different abundances between patients with ATLL and healthy controls ($P = 0.05$). Among these KOs, 463 were significantly more abundant in the ATLL patient group than in the control group. These KOs were present in more than 14 individuals in the ATLL patient group (representing approximately 80 % of the patients with ATLL) ($P = 0.05$; Fig. 5A). To determine which pathways are involved in these KOs, enrichment analysis was performed using Enteropathway [23], a map specific to metabolic pathways and modules in the human gut microbiome. Enrichment analysis revealed 12 upregulated metabolic modules in patients with ATLL ($P < 0.05$), and three modules had Q values less than 0.05 after FDR correction (Fig. 5B, Supplementary Fig. S8). We also conducted enrichment analysis for the 154 KOs, the abundances of which were significantly lower in the gut microbiome of patients with ATLL than in that of controls (Supplementary Fig. S9).

Of the three significantly enriched modules, we focused on the homoprotocatechuate (HPC) degradation module (Fig. 5B and C)

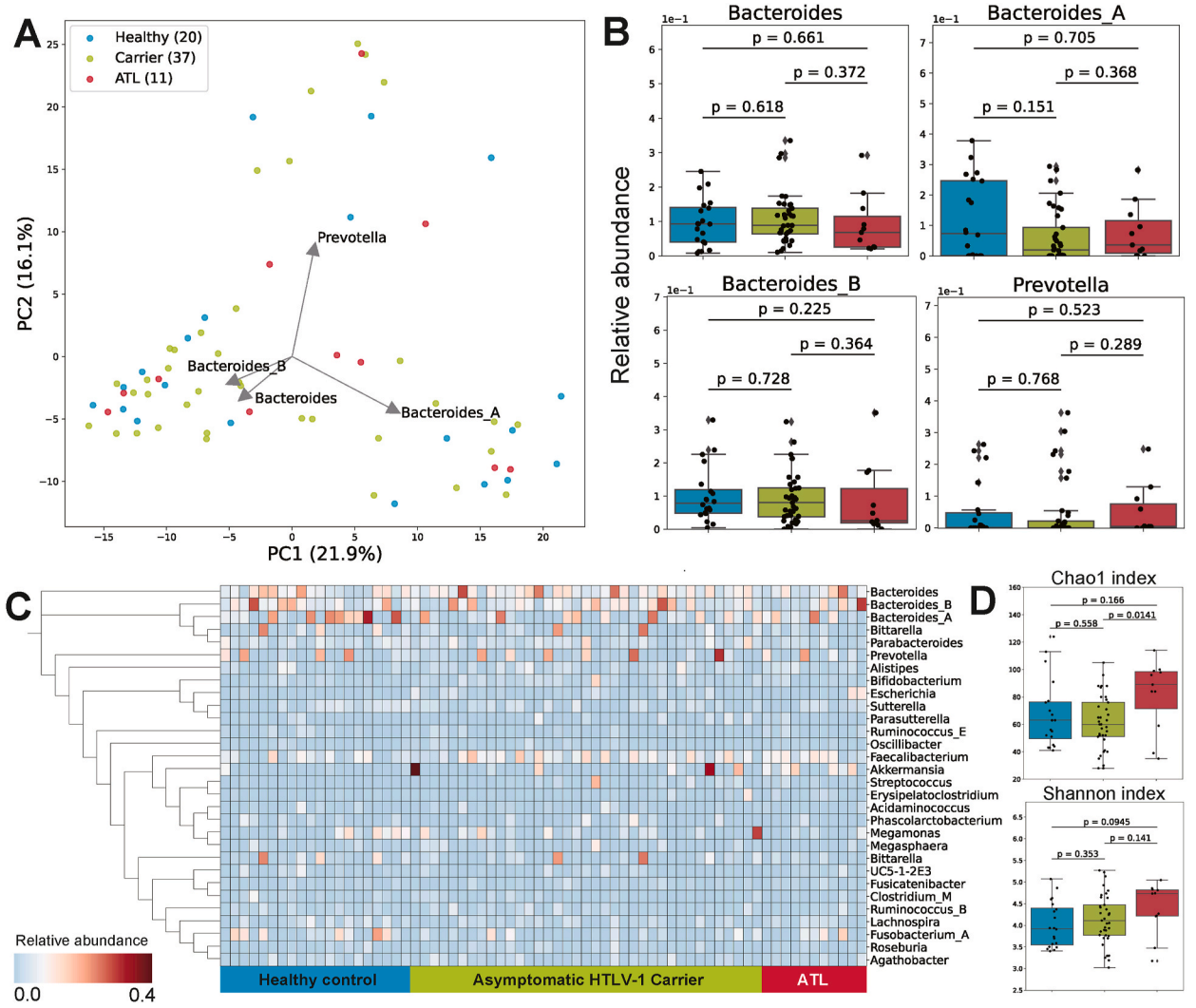

Fig. 2. Comparison of the gut microbial community structure between patients with ATLL and asymptomatic HTLV-1 carriers.
Blue, healthy controls; green, asymptomatic HTLV-1 carriers; red, patients with ATLL.
(A) PCA plot of the subjects' gut microbiota taxonomic composition.
(B) Variation in the relative abundance of the four dominant genera in the subjects' guts. P values were calculated by the two-tailed Brunner–Munzel test.
(C) Relative abundance of the top 30 genera in patients with ATLL, asymptomatic HTLV-1 carriers, and healthy controls. A phylogenetic tree was constructed from 16S rRNA gene sequences.
(D) Alpha diversity of the subjects' gut microbiota. P values were calculated by the two-tailed Mann−Whitney *U* test. The Shannon index did not significantly differ among all the groups.

because succinic semialdehyde (SSA), the end product of the module, is considered to lead to oxidative stress, and oxidative stress is known to be involved in the development of tumors [24,25].

Klebsiella and *Escherichia* were the main genera associated with the module (Fig. 5D, right bar graph), which is consistent with findings from previous reports [26–28]. The gut microbiota associated with the other two significantly enriched modules are shown in Supplementary Figs. S10 and S11.

Finally, to demonstrate the impact of SSA on ATLL cell lines, we treated three types of leukemia cell lines (MT-1, ILT-Mat, and ATN cells) derived from patients with ATLL with various concentrations of SSA for three days (Fig. 5E and F; Supplementary Fig. S12). We measured cell proliferation based on the absorbance values. We observed that, compared with the control, 200 μM SSA significantly promoted the proliferation of ATLL cell lines, which was not dependent on IL-2. Thus, these findings suggest that SSA promotes the proliferation of the ATLL cells and that *Klebsiella* may contribute to this effect.

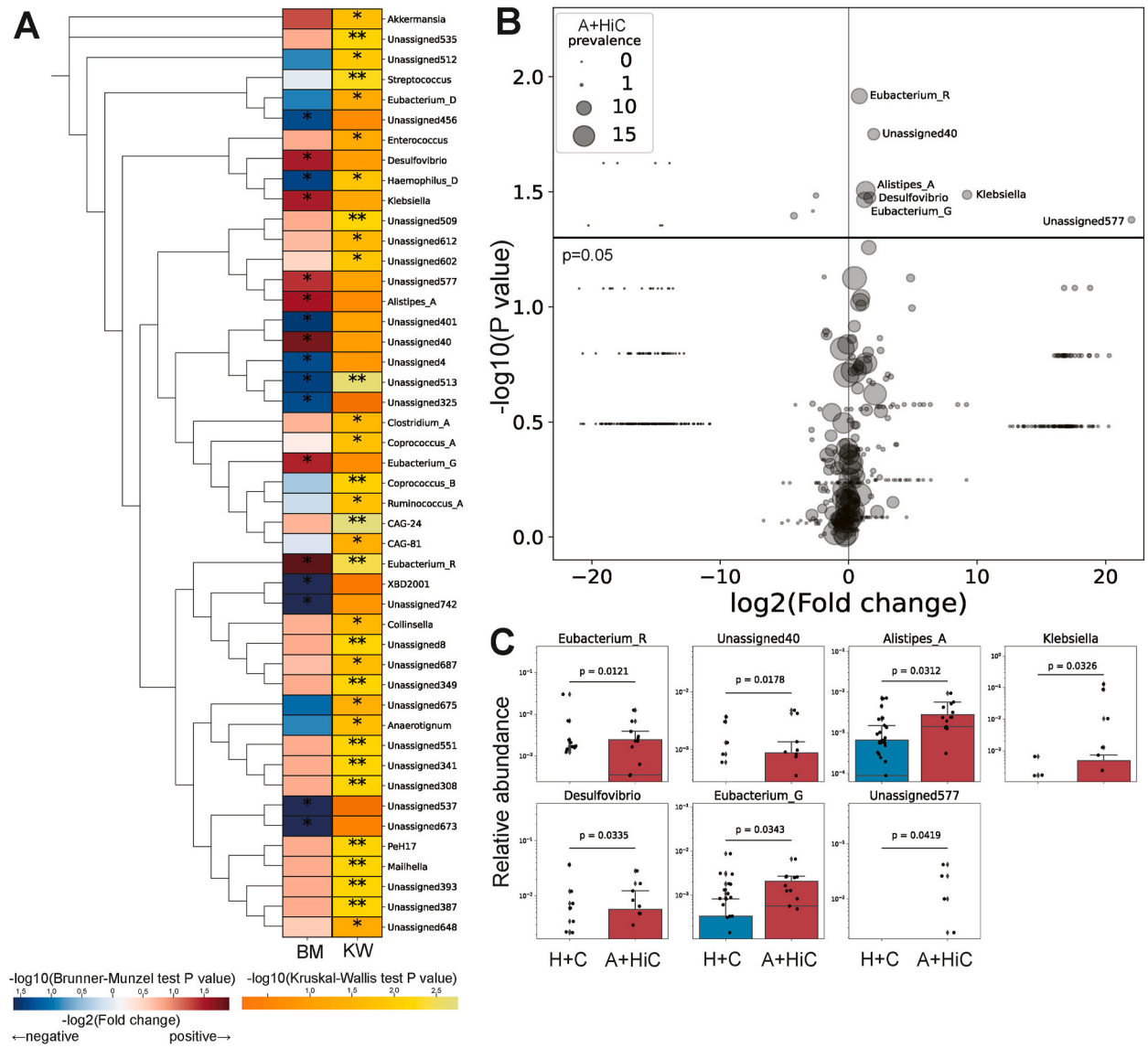

Fig. 3. Differential analysis of the abundance of each genus in the gut microbiota.
A + HiC, a combined group of patients with ATLL and high-risk HTLV-1 carriers; H + C, a combined group of healthy controls and asymptomatic HTLV-1 carriers.
(A) The distribution of P values for 46 bacterial genera with significant differences in abundance according to the two-tailed Brunner–Munzel test (left column, "BM") and Kruskal–Wallis test (right column, "KW"). Bacteria with significantly increased abundance compared to H + C are represented as red, and those with decreased abundance are represented as blue on the left side of the heatmap. The color intensity reflects the magnitude of the -$\log_{10}$ (P value). *, $P < 0.05$; **, $P < 0.01$. A phylogenetic tree was constructed from the V3-V4 region of the 16S rRNA gene sequences.
(B) Comparison of the abundance of each bacterial genus between the A + HiC and H + C groups. The X-axis represents the ratio of the mean relative abundance of each group (fold change) transformed by $\log_2$; the Y-axis represents the P value transformed by -$\log_{10}$. The horizontal line represents $P = 0.05$. P values were calculated by the two-tailed Brunner–Munzel test. The plot size represents the prevalence of each bacterium (number of subjects) in the A + HiC group.
(C) The relative abundance of seven genera was significantly greater in the A + HiC group (red) than in H + C group (blue). P values were calculated by the two-tailed Brunner–Munzel test.

3. Discussion

In this study, we investigated the variations in the gut microbiome of patients with ATLL and asymptomatic HTLV-1 carriers using *in vitro* and *in silico* analyses. Our findings suggest a potential role for the gut microbiome and metabolites in ATLL progression. This study is one of the few to explore the link between hematological tumors and the gut microbiome, shedding light on the mechanism of

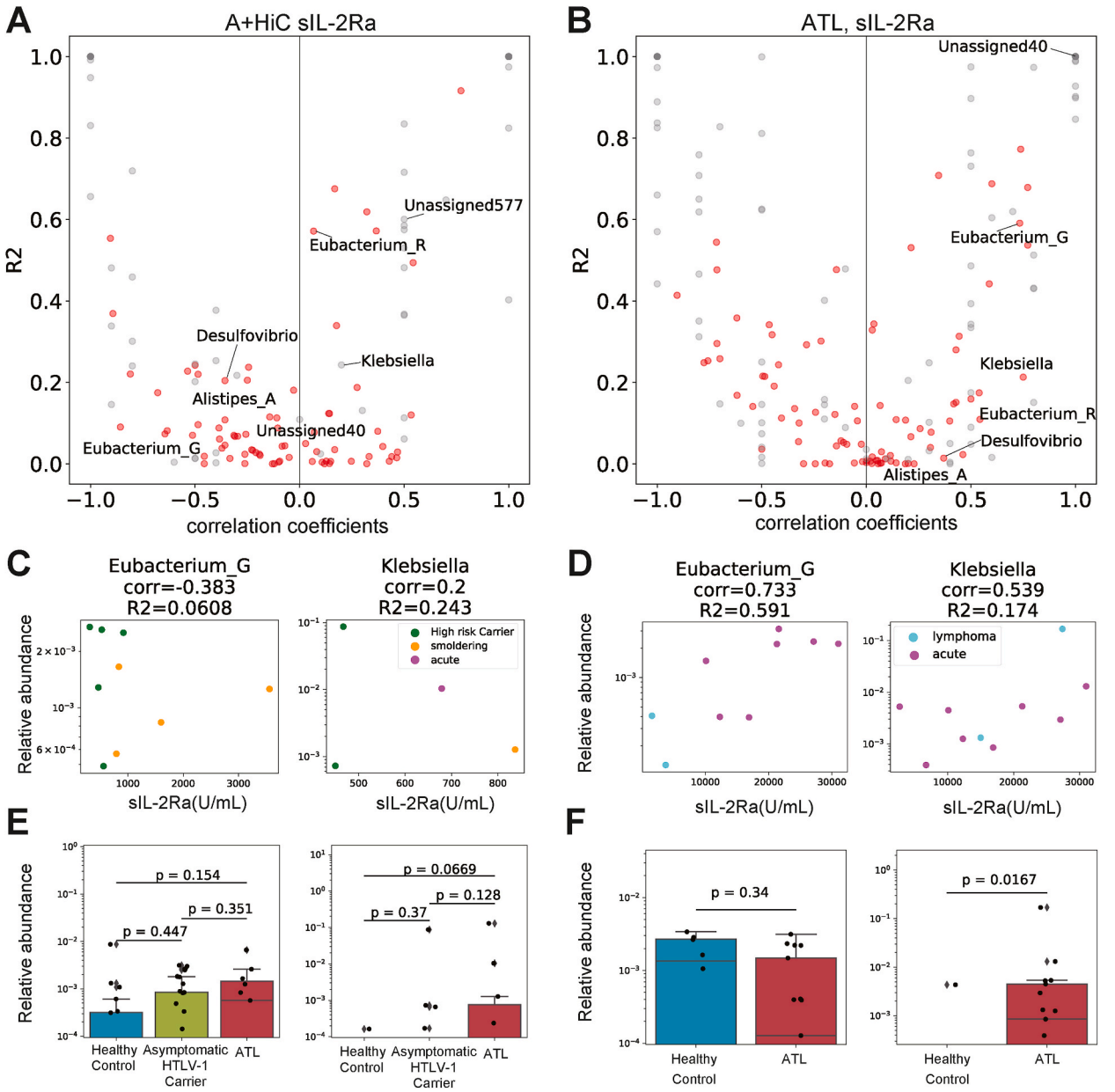

Fig. 4. Correlations between tumor markers and the relative abundance of each bacteria.
(A), (B) Distribution of Spearman correlation coefficients between sIL-2Ra levels and the relative abundance of each individual bacteria (X-axis) and the R^2 score (Y-axis) for patients with ATLL and high-risk HTLV-1 carriers in cohort 1 (A) and cohort 2 (B). The bacterial names in the figure represent the bacterial genera whose abundance increased with the progression of ATLL identified in the previous section. Red plots represent bacteria that were found in five or more subjects; subjects had measurable bacterial abundance values and sIL-2Ra levels. A relative abundance of 0 was omitted before the correlation coefficient was calculation.
(C), (D) The distribution of sIL-2Ra levels (X-axis) and relative abundance (Y-axis) of *Eubacterium_G* (left) and *Klebsiella* (right). The relative abundance values were converted by $\log_{10}$. Corr, Spearman's correlation coefficient: R2, coefficient of determination. The plot color represents ATLL subtypes: green, high-risk HTLV-1 carrier; yellow, smoldering type; pink, acute type; and cyan, lymphoma type. (C) Patients with ATLL and high-risk HTLV-1 carriers in cohort 1 and (D) patients with ATLL in cohort 2.
(E), (F) The relative abundance of *Eubacterium_G* (left) and *Klebsiella* (right). The relative abundance values were converted by $\log_{10}$. P values were calculated by the two-tailed Brunner–Munzel test. (E) Cohort 1 and (F) cohort 2.

tumor progression.

We observed an increased abundance of *Klebsiella* and other genera in high-risk HTLV-1 carriers and patients with ATLL (Fig. 3C), which was positively correlated with tumor marker levels of patients with ATLL (Fig. 4D). Notably, our metagenomic data revealed

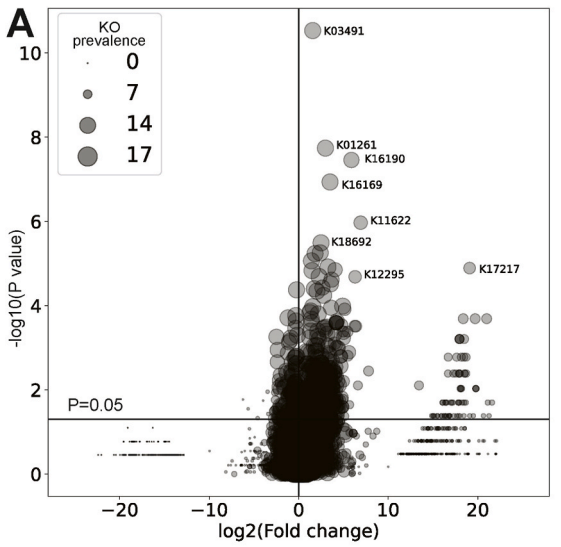

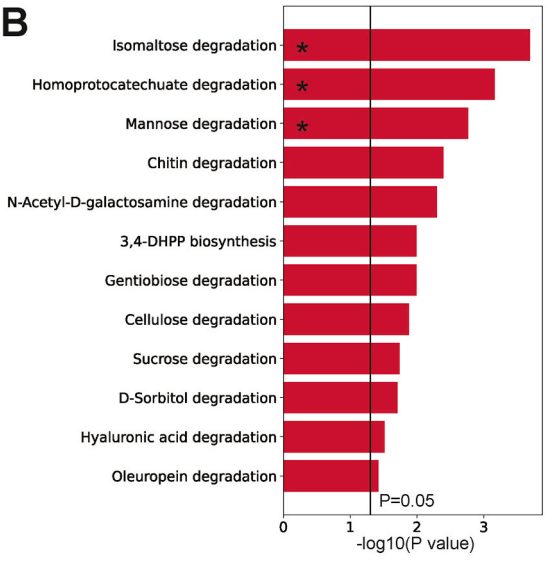

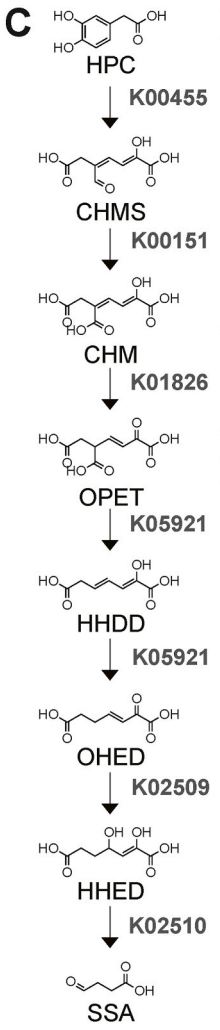

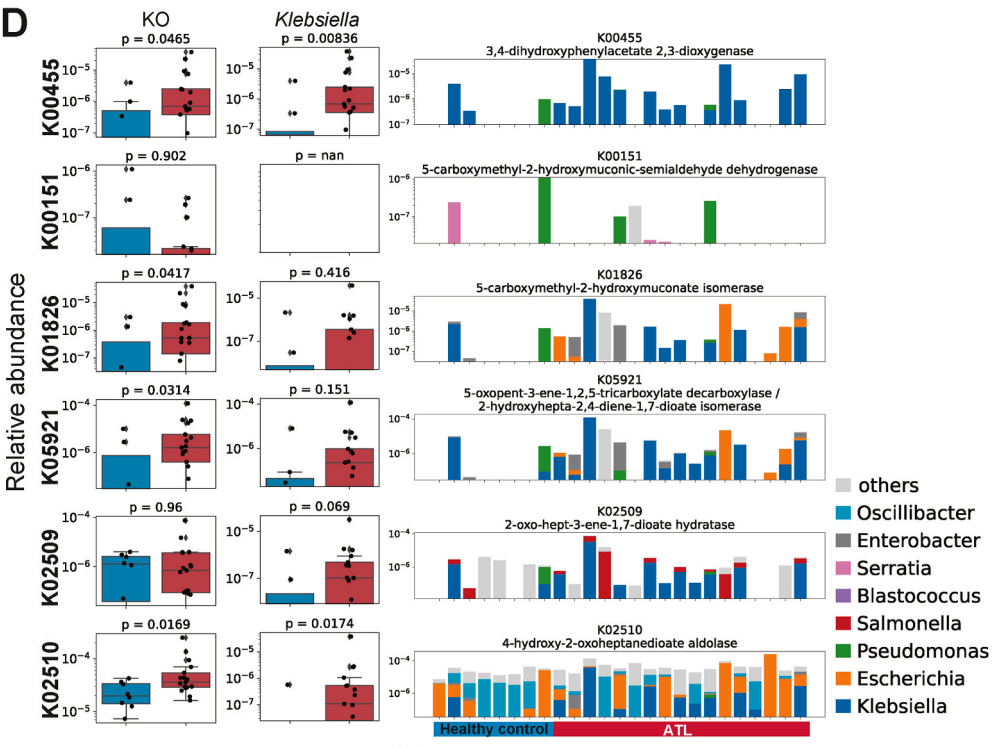

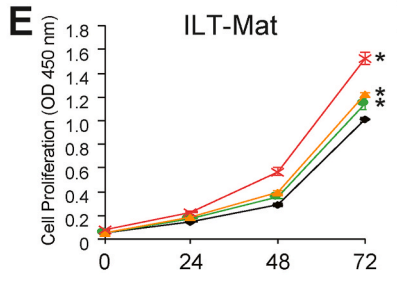

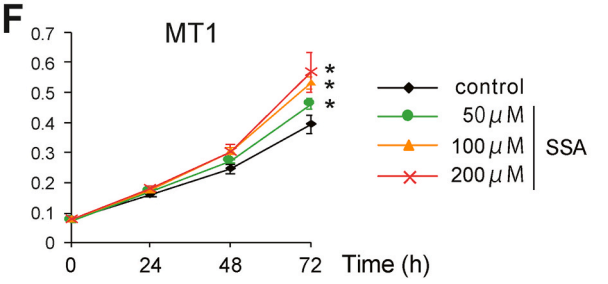

(caption on next page)

Fig. 5. Gut microbial functional modules with altered abundance in the ATLL patient group.
(A) Comparison of KO abundances between patients with ATLL and healthy controls. X-axis, fold change (log_2-transformed) in the mean relative abundance of each bacterium in each group; Y-axis, -log_{10}-transformed P values from pairwise comparisons. The horizontal line represents P = 0.05. P values were calculated by the two-tailed Brunner–Munzel test. The plot size shows the KO prevalence (number of subjects) in the ATLL patient group.
(B) Enrichment analysis of KOs that were significantly more abundant in patients with ATLL. P values are transformed by -log_{10}. The vertical line represents P = 0.05. *, q < 0.05.
(C) SSA synthesis module. Abbreviations: HPC, homoprotocatechuate; CHMS, 5-carboxymethyl-2-hydroxymuconic-semialdehyde; CHM, 5-carboxymethyl-2-hydroxymuconate; OPET, 5-oxo-pent-3-ene-1,2,5-tricarboxylate; HHDD, 2-hydroxyhepta-2,4-diene-1,7-dioate; OHED, 2-oxo-hept-3-ene-1,7-dioate; HHED, 2,4-dihydroxy-hept-2-ene-1,7-dioate; SSA, succinic semialdehyde.
(D) Association of KO abundance and genus *Klebsiella* with the SSA synthesis module. The box plot represents the relative abundance of the KOs (left) and ortholog genes assigned to the KO from *Klebsiella* (right). The bar plot represents the bacterial composition of the KOs of each subject (right). The top two genera with the highest average relative abundance in at least one KO are displayed.
(E) (F) Cell growth rate. (E) IL-2-dependent ILT-Mat cells and (F) IL-2-independent MT-1 cells treated with SSA. The values represent the means ± s.d. *P < 0.05; unpaired two-tailed Student's *t*-test.

enrichment of SSA synthesis pathway in the gut microbiota, particularly *Klebsiella* was a main contributor of it in the guts of patients with ATLL (Fig. 5B–D). We confirmed that SSA promoted the proliferation of ATLL cells (Fig. 5E and F). Overall, our study provides insights into the potential involvement of the gut microbiota in ATLL progression.

Antibiotics increase *Klebsiella* abundance [3] and cause dysbiosis of the gut microbiota [29]. Indeed, most patients with ATLL in this study had a history of antibiotic use within one week of fecal collection. It is possible to hypothesize that antibiotics might induce ATLL by increasing *Klebsiella* abundance and worsen ATLL by disrupting the gut microbiota. However, this remains a hypothesis, and further analyses, such as tracking the gut microbiota of ATLL patients before and after antibiotic treatment over time, are necessary. In addition, a species in the genus *Klebsiella* is also known to cause opportunistic infections [3]. Previous reports have suggested that *S. stercoralis* antigens may promote ATLL via IL-2 activation [30,31]. Therefore, the increasing abundance of *Klebsiella* may alter the host immune system in the gut, affecting ATLL development.

SSA is known to be a reactive carbonyl and may induce oxidative stress in cells. Oxidative stress can cause tumor expansion [25]. A previous study reported that HTLV-1 Tax-expressing cells showed antiapoptotic property under oxidative stress [32]. These findings suggest that oxidative stress caused by SSA may lead to ATLL progression via ATLL cell proliferation. In other words, it is possible that SSA is a potential driver of ATLL. However, another study showed that Tax itself stimulates reactive oxidative stress (ROS) production and induces the apoptosis of T cells [33]. In addition, Tax expression is temporary, and more than half of HTLV-1-infected cells do not express Tax [32]. Thus, the mechanism of ATLL cell proliferation by oxidative stress and SSA needs to be determined.

Based on our findings and those of previous studies, we propose a hypothesis for ATLL development and progression. An increase in the abundance of gut *Klebsiella* leads to enhanced homoprotocatechuate degradation, resulting in elevated SSA concentrations and promoting ATLL cell expansion (Fig. 6).

Several limitations exist in our study. First, the SSA concentration in the intestinal tract or peripheral blood due to increased homoprotocatechuate degradation by *Klebsiella* still needs to be better understood. Measurement of the SSA concentration in patients with ATLL and SPF ATLL model animals colonized by *Klebsiella* is needed. Second, several subjects had a history of illness or treatment (antibiotics or chemotherapy) before fecal sampling, potentially influencing the study outcome. Analysis of untreated, sex- and age-unbiased samples is needed, but no associations between increased *Klebsiella* abundance and antibiotic/chemotherapy history or age- or sex-related bias were found in this study (data not shown). Taken together, further experiments and analyses that address these limitations will provide additional evidence about the association between the gut microbiome and ATLL progression.

4. STAR methods

Key resource table

REAGENT or RESOURCE	SOURCE	IDENTIFIER
Biological samples		
Human gut microbial DNA from fecal samples	This study	N/A
Chemicals, peptides, and recombinant proteins		
RPMI-1640 medium	FUJIFILM Wako Pure Chemical Corporation	18902025
fetal bovine serum	Cosmobio	3031 CCP-FBS-BR-500
Penicillin- streptomycin	FUJIFILM Wako Pure Chemical Corporation	168-23191
nonessential amino acids	FUJIFILM Wako Pure Chemical Corporation	13915651
interleukin-2	BioLegend	589104
succinic semialdehyde	Santa Cruz Biotechnology	sc-281158
Critical commercial assays		
WST-8 method with a Cell Counting Kit	Dojindo	341-07624

(*continued on next page*)

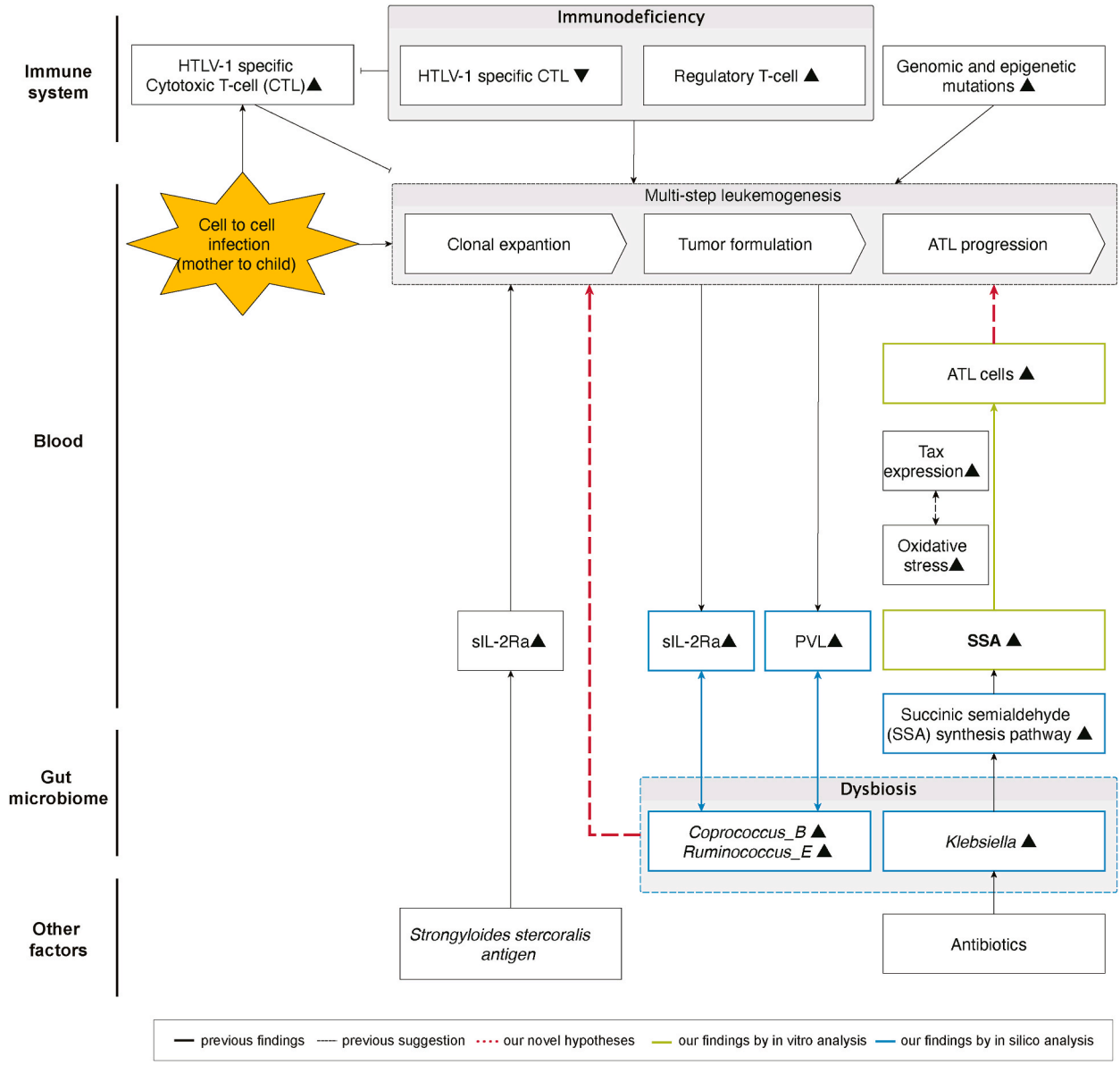

Fig. 6. Hypotheses and previous findings on the mechanism of development and progression of ATLL.
We summarized our hypotheses and previous findings related to the development and progression of ATLL.

(*continued*)

REAGENT or RESOURCE	SOURCE	IDENTIFIER
preservation solution kit of fecal sample	Technosuruga	
PowerFecal DNA Isolation Kit	QIAGEN	12830-50
QIAmp DNA Stool	QIAGEN	51504
Deposited data		
Raw and analyzed gut bacterial DNA sequence data	This paper	DNA Data Bank of Japan (DDBJ) Sequence Read Archive (DRA), DRA016992.
Experimental models: Cell lines		
MT-1	JCRB CELL BANK	JCRB
ILT-Mat	RIKEN BRC CELL BANK	RCB0475
ANT	RIKEN BRC CELL BANK	RCB1440
Oligonucleotides		

(*continued on next page*)

(*continued*)

REAGENT or RESOURCE	SOURCE	IDENTIFIER
16S rRNA-Forward Primer 341F: 5′- TCGTCGGCAGCGTCAGATGTGTATAAGAGACAGNCCTACGGGNGGCWGCAG-3′	Oral Microbiome Center, Taniguchi Dental Clinic	N/A
16S rRNA-Reverse Primer −806R: 5' – GTCTCGTGGGCTCGGAGATGTGTATAAGAGACAGNGACTACHVGGGTATCTAATCC-3′	Oral Microbiome Center, Taniguchi Dental Clinic	N/A
Software and algorithms		
Fastp	Chen et al. [34]	https://github.com/OpenGene/fastp
VSEARCH	Rognes et al. [35]	https://github.com/torognes/vsearch
SeqKit	Shen et al. [36]	https://github.com/shenwei356/seqkit/releases
Deblur	Amir et al. [37]	https://github.com/biocore/deblur
SortMeRNA	Kopylova et al. [38]	https://github.com/sortmerna/sortmerna
BLASTn	Camacho et al. [39]	https://blast.ncbi.nlm.nih.gov/Blast.cgi
Cutadapt	Marcel [40]	https://github.com/marcelm/cutadapt
Bowtie2	Langmead et al. [41]	http://bowtie-bio.sourceforge.net/bowtie2/index.shtml
MEGAHIT	Li et al. [42]	https://github.com/voutcn/megahit
Prodigal	Hyatt et al. [43]	https://github.com/hyattpd/Prodigal
MMseqs2	Steinegger et al. [44]	https://github.com/soedinglab/MMseqs2
Diamond	Buchfink et al. [45]	https://github.com/bbuchfink/diamond
MAFFT	Katoh et al. [46]	https://mafft.cbrc.jp/alignment/software/
RAxML	Stamatakis et al. [47]	https://github.com/amkozlov/raxml-ng
iTOL	Letunic et al. [48]	https://itol.embl.de/
Enteropathway	Shiroma et al. [23]	https://enteropathway.org/#/
Other		
GTDB	Donovan et al. [49]	https://gtdb.ecogenomic.org/
MGnify	Mitchell et al. [50]	https://github.com/EBI-Metagenomics
Python	Python Software Foundation	https://www.python.org/downloads/release/python-376/

5. Resource availability

This study did not generate new unique reagents.

6. Data availability statement

6.1. Data

The raw sequencing data reported in this paper have been deposited in the DNA Data Bank of Japan (DDBJ) Sequence Read Archive (DRA), Tokyo, Japan, under accession number DRA016992.

6.2. Code

This paper does not report the original code.

6.3. Experimental model and study participant details

6.3.1. In vitro experiments

ATLL patient-derived leukemia cell lines (MT-1, ATN-1, and ILT-Mat) were procured from the JCRB or RIKEN cell bank in 2022. The cell lines were authenticated utilizing STR-PCR profiling and tested negative for mycoplasma. MT-1 cells were cultured in RPMI-1640 medium (Fujifilm Wako Pure Chemical Corporation, Osaka, Japan) supplemented with 10 % fetal bovine serum (Cosmobio, Tokyo, Japan), penicillin (100 U/ml), and streptomycin (100 μg/ml) (Fujifilm Wako Pure Chemical Corporation, Osaka, Japan) (complete RPMI-1640 medium). ATN-1 and ILT-Mat cells were cultured in complete RPMI-1640 medium supplemented with 1 ×

nonessential amino acids (Fujifilm Wako Pure Chemical Corporation, Osaka, Japan) and interleukin-2 (BioLegend, San Diego, USA), respectively. The cells were maintained at 37 °C in a humidified atmosphere with 5 % CO_2.

Cells were seeded into 96-well plates at densities ranging from 50×10^3 to 200×10^3 cells in 100 μL of complete cell culture medium, and succinic semialdehyde (Santa Cruz Biotechnology, Texas, USA) was added to the medium for 72 h at 37 °C with 5 % CO_2. Cell proliferation was assessed every 24 h using the WST-8 method with a Cell Counting Kit (Dojindo, Kumamoto, Japan) following the manufacturer's instructions. The experiments were performed in triplicate and repeated at least three times.

6.3.2. Study participants' sample collection

The Miyazaki University Faculty of Medicine Ethics Committee and participating institution approved the study (approved number 2020-565). Samples and clinical information were obtained with informed consent. Patients with ATLL and asymptomatic HTLV-1 carriers aged over 20 years old with confirmed HTLV-1 infection were recruited from Miyazaki University Hospital and Imamura General Hospital in Japan. Healthy controls aged over 20 years old with no family history of ATLL were recruited. We obtained fecal samples from two cohorts because fecal samples were collected from asymptomatic HTLV-1 carriers at home after the hospital visit using a preservation solution kit [18], while fresh fecal samples were collected from patients with ATLL at the same time as hospital admission. Therefore, one cohort included asymptomatic HTLV-1 carriers (n = 37) and patients with less advanced types of ATLL (n = 11), such as the smoldering type and healthy controls (n = 20) (cohort 1, Table 1). In the asymptomatic HTLV-1 carrier group, there were eight asymptomatic HTLV-1 carriers with HTLV-1 proviral loads (PVLs) above 40 (per 1000 peripheral blood mononuclear cells (PBMCs)), and we defined them as high-risk carriers [19]. The other cohort included patients with advanced-stage ATLL, such as acute type (n = 17), and healthy controls (n = 8) (cohort 2, Table 2). In cohort 1, patients with ATLL were significantly older (Mann–Whitney *U* test, two-tailed, P = 0.00164 vs. asymptomatic HTLV-1 carriers, $P = 1.39 \times 10^{-9}$ vs. healthy controls). There were more women in the asymptomatic HTLV-1 carrier group than in the control group, whereas the healthy controls were all men. In cohort 2, patients with ATLL were significantly older than healthy controls ($P = 3.89 \times 10^{-19}$).

The soluble interleukin 2 receptor-alpha (sIL-2Ra) levels, PVL levels, and clinical data were collected from the medical records (Table 1). sIL-2Ra is a blood biomarker that reflects tumor size and disease progression in patients with ATLL. sIL-2Ra also reflects lymphoma and other immune disorders, but none of the study subjects had these diseases. The samples and clinical information used in this study were obtained after providing informed consent and with the approval of the institutional review boards of each participating institute of the University of Miyazaki.

7. Method details

7.1. 16S rRNA gene sequencing

To obtain 16S rRNA gene sequencing data from cohort 1, DNA was extracted from fecal samples with preserved guanidine solution using the PowerFecal DNA Isolation Kit (QIAGEN, Hilden, Germany). To obtain 16S rRNA gene sequencing data from cohort 2, DNA was extracted from fresh fecal samples using the QIAmp DNA Stool (QIAGEN, Hilden, Germany). After extraction, the libraries were prepared following the official Illumina protocol for 16S Metagenomics Sequencing Library Preparation.

The V3-V4 region of the 16S rRNA gene was amplified using 341F-806R primers and KAPA HiFi HotStar (Nippon Genetics, Tokyo, Japan). The resulting DNA was purified with AMpureXP (Nippon Genetics, Tokyo, Japan) and subjected to two washes with 80 % ethanol, followed by elution with 10 mM Tris buffer (pH 8.5). The resulting library was denatured with 0.2 N NaOH after adjusting to 4 nM and HT1 buffer, and paired-end sequencing was performed using MiSeq with the addition of 20 % 10 pM PhiX DNA (Oral Microbiome Center, Taniguchi Dental Clinic, Kagawa, Japan). On average, 197,008 reads were obtained per sample.

7.2. Shotgun metagenomic sequencing

For whole-genome shotgun sequencing data acquisition, DNA was extracted from fecal samples stored at 4 °C using a QIAamp DNA Stool (QIAGEN, Hilden, Germany) within 24 h. One stool sample from a patient with ATLL was stored at 4 °C for five days before DNA extraction. PCR was performed according to the official Illumina protocol for the Nextera DNA Flex Library preparation kit five times after DNA fragmentation. Subsequently, 12 pM PhiX DNA was added at 5 %, and sequencing was subsequently conducted on a NovaSeq instrument. On average, 143,084,977 reads were obtained per sample (Oral Microbiome Center, Taniguchi Dental Clinic, Kagawa, Japan).

7.3. Taxonomic profiling

To estimate the phylogenetic composition, we utilized the reads obtained from 16S rRNA gene sequence data and processed them through our in-house pipeline (Supplementary Fig. S1). Fastp (version 0.19.6) [34] was used for quality filtering, which involved removing adaptor sequences, poly G sequences longer than 10 base pairs, reads shorter than 200 base pairs, reads containing one or more undetermined nucleotides (N) from the sequencer, and reads with an average quality score lower than 15.

Next, VSEARCH (version 2.7.0_linux_x86_64) [35] was used to combine forward and reverse reads, resulting in an average of 136, 908.7 high-quality reads per sample. The length distribution of these reads was examined with SeqKit (version 0.5.5)[36] and the reads were trimmed to 400 base pairs using the deblur trim command in Deblur (version 1.1.0-dev) [37]. Duplicate reads were counted, and singletons were removed with the deblur dereplicate command. PhiX-derived reads were eliminated with the deblur remove-artifacts

command using a file of PhiX sequences registered in Deblur and converted with SortMeRNA (version 2.0)[38]. Multiple sequence alignments were conducted with the deblur multiple-seq-alignment command to detect sequencing errors, followed by denoising with the deblur deblur-seqs command. Finally, the uchime_denovo command with VSEARCH was used to remove chimeric sequences generated during read merging. After all these steps, a total of 6,838 reads (ASVs) were retrieved.

Phylogenetic assignments for these reads were obtained from the GTDB (https://data.gtdb.ecogenomic.org/releases/release86/86.1/bac120_ssu_r86.1.fna) [49]. BLASTn (version 2.8.1) [39]was utilized for homology searches. Genus names were assigned from identity $\geq$ 94 % match to registered sequences, while species names were assigned with an identity $\geq$ 99 % match to reference sequences. Ultimately, 6,093 reads were assigned a phylogenetic name above the genus level (Supplementary Fig. S1).

7.4. Functional profiling

To estimate the functional composition, we used the reads obtained from whole-genome shotgun sequencing data (Supplementary Fig. S2). For quality filtering, we first removed adaptor sequences from the forward and reverse reads by using Cutadapt (version 1.9.1)[40]. The command for forward reads was as follows:

cutadapt -a CTGTCTCTTATACACATCTCCGAGCCCACGAGAC -O 33

The command for reverse reads was as follows:

cutadapt -a CTGTCT CTTATACACATCTGACGCTGCCGACGA -O 32

Fastp was subsequently used to remove poly G sequences longer than 10 base pairs, reads shorter than 200 base pairs, reads containing one or more undetermined bases (N) from the sequencer, and reads with an average quality score lower than 15. PhiX and human-derived DNA sequences were removed using Bowtie2 (version 2.2.9)[41]. Only paired-end reads were counted, resulting in a total of 141,279,674 high-quality reads.

MEGAHIT (version 1.1.1–2) [42] was used for assembly, in which contigs were created. Mapping of high-quality reads to the contigs was performed using Bowtie2. Gene prediction for the contigs was accomplished using Prodigal (version 2.6.3) [43] to obtain amino acid sequences. Representative sequences were obtained by clustering sequences with 100 % similarity using MMseq2 (version 61ca48883b50714be51fc35fc9b77325ffde53fb) [44]. Functional assignment was performed through a homology search with the representative sequence using DIAMOND (version 0.9.10) [45] against the Unified Human Gastrointestinal Protein (UHGP) catalog in the MGnify (version 2019.8)[50]. The abundance of functional genes was calculated based on sequence identity >40, bit score >70, and coverage >80, matching the list of genes assigned to the gene name of the UHGP with the mapping output. Additionally, the abundance of orthologs was calculated using the Kyoto Encyclopedia of Genes and Genomes (KEGG) Orthology (KO) [51] linked to the UHGP of MGnify. The results revealed 4,287,107 assigned genes and 7,861 KOs (Supplementary Fig. S2).

The contribution (abundance) of each bacterium to each KO was calculated from the output of the UHGP gene profile. The gene profile included the ID of each gene, the strain name of the bacteria containing that gene, and the ID of the KO.

7.5. Phylogenetic tree

For phylogenetic tree estimation, the 16S rRNA amplicon sequences of all the strains belonging to the genera were aligned using MAFFT [46]. RAxML [47] was subsequently used to construct the phylogenetic tree, the parameters of which were set to raxmlHPC-SSE3 -m GTRGAMMA -p 12345. The visualization of the tree was performed using iTOL [48].

7.6. Statistical analysis

To calculate the fold change in the mean abundance of each microbe, 1.0×10^{-9} was added to all the bacterial relative abundance values. For the fold change in KOs, 1.0×10^{-12} was added to all the KO abundance values.

Principal component analysis (PCA) was performed on the relative abundance of each bacterial strain using the sklearn.decomposition module of scikit-learn in Python (version 3.9.7). The relative abundances were converted to z scores using scipy stats.

For two-group comparisons of bacterial and KO abundances, two-sided Brunner–Munzel tests were used. The significance level for bacterial and KO abundance comparisons was set at $p = 0.05$. In this analysis, the significance level was set at $p = 0.05$ unless otherwise mentioned. Additionally, statistical significance was determined by using the following tests:

1. Two-sided Mann–Whitney *U* test to determine differences in demographic information and alpha diversity between groups.
2. Two-sided Brunner-Munzel tests to determine differences in the bacterial and KO abundances between groups.
3. Two-sided Kruskal–Wallis test to determine differences in bacterial abundance between the four groups.

For correlation analysis between bacterial abundance and blood biomarker values, the Spearman correlation coefficient was used. The goodness of fit of the correlation coefficient was assessed using the coefficient of determination (R^2 score). Enrichment analysis was performed using Enteropathway [23]. This analysis focused on the KOs with significant differences in abundance between the ATLL patient group and healthy controls. The significance level for this analysis was set at $p = 0.05$.

Ethics statements

This study was reviewed and approved by Miyazaki University with the approval number: 2020-565, dated March 16, 2021.

All participants provided written informed consent to participate in the study and for their data to be published.

Grant support

This work was supported by grants from the Japan Society for the Promotion of Science (JJSPS) KAKENHI (19K07693, 22K07172 to S.Nakahata; 15K15087 to K.M.; JP16H06279 (PAGS) to T.Y.), the Japan Agency for Medical Research and Development (JP21ck0106546h0002, JP21cm0106477, JP22ama221404) (to T.Y.), Japan Science and Technology Agency AIP Acceleration Research (JPMJCR19U3) (to T.Y.), and JST SPRING (JPMJSP2106) (to N.C.).

CRediT authorship contribution statement

Nodoka Chiba: Writing – review & editing, Writing – original draft, Validation, Investigation, Funding acquisition, Formal analysis, Data curation, Conceptualization. **Shinya Suzuki:** Investigation. **Daniel Enriquez-Vera:** Investigation. **Atae Utsunomiya:** Resources. **Yoko Kubuki:** Resources. **Tomonori Hidaka:** Resources. **Kazuya Shimoda:** Resources. **Shingo Nakahata:** Writing – review & editing, Writing – original draft, Validation, Supervision, Resources, Investigation, Funding acquisition, Formal analysis, Conceptualization. **Takuji Yamada:** Writing – review & editing, Writing – original draft, Validation, Supervision, Investigation, Funding acquisition, Formal analysis, Conceptualization. **Kazuhiro Morishita:** Writing – review & editing, Validation, Supervision, Investigation, Funding acquisition, Formal analysis, Conceptualization.

Declaration of competing interest

The authors declare the following financial interests/personal relationships which may be considered as potential competing interests:Takuji Yamada reports a relationship with Metagen Therapeutics Inc that includes: board membership. Takuji Yamada reports a relationship with Metagen Inc that includes: board membership. If there are other authors, they declare that they have no known competing financial interests or personal relationships that could have appeared to influence the work reported in this paper.

Acknowledgments

We would like to thank all the participants and their families who participated in this study. We thank Dr. Hirotsugu Shiroma (Tokyo Institute of Technology) for constructing the whole-genome shotgun metagenomic sequence pipeline. We would also like to acknowledge Dr. Chikako Tani (University of Miyazaki) and Ms. Satomi Harazono (Kagoshima University) for providing research assistance. We would like to thank Dr. Sayaka Mizutani (Tokyo Institute of Technology) for advice on the paper-writing technique.

Appendix A. Supplementary data

Supplementary data to this article can be found online at https://doi.org/10.1016/j.heliyon.2024.e38507.

References

[1] K. Hou, Z.X. Wu, X.Y. Chen, J.Q. Wang, D. Zhang, C. Xiao, D. Zhu, J.B. Koya, L. Wei, J. Li, et al., Microbiota in health and diseases, Signal Transduct. Targeted Ther. 71 (7) (2022) 1–28, https://doi.org/10.1038/s41392-022-00974-4, 2022.
[2] G. Dalmasso, A. Cougnoux, J. Delmas, A. Darfeuille-Michaud, R. Bonnet, The bacterial genotoxin colibactin promotes colon tumor growth by modifying the tumor microenvironment, Gut Microb. 5 (2014) 675–680, https://doi.org/10.4161/19490976.2014.969989.
[3] N. Raffelsberger, M.A.K. Hetland, K. Svendsen, L. Småbrekke, I.H. Löhr, L.L.E. Andreassen, S. Brisse, K.E. Holt, A. Sundsfjord, Ø. Samuelsen, et al., Gastrointestinal carriage of Klebsiella pneumoniae in a general adult population: a cross-sectional study of risk factors and bacterial genomic diversity, Gut Microb. 13 (2021), https://doi.org/10.1080/19490976.2021.1939599.
[4] R. Wang, X. Yang, J. Liu, F. Zhong, C. Zhang, Y. Chen, T. Sun, C. Ji, D. Ma, Gut microbiota regulates acute myeloid leukaemia via alteration of intestinal barrier function mediated by butyrate, Nat. Commun. 131 13 (2022) 1–18, https://doi.org/10.1038/s41467-022-30240-8, 2022.
[5] A. Allegra, V. Innao, A.G. Allegra, R. Ettari, M. Pugliese, N. Pulvirenti, C. Musolino, Role of the microbiota in hematologic malignancies, Neth. J. Med. 77 (2019) 67–80.
[6] C. Niemann, M. Coelho, S. Öztürk, M. Seiffert, The Diversity of the Microbiome Impacts Chronic Lymphocytic Leukemia Development in Mice and Humans, 2023, https://doi.org/10.21203/RS.3.RS-3184540/V1.
[7] T. Ma, Y. Chen, L.J. Li, L.S. Zhang, Opportunities and challenges for gut microbiota in acute leukemia, Front. Oncol. 11 (2021) 692951, https://doi.org/10.3389/FONC.2021.692951/BIBTEX.
[8] A.A. Phillips, J.C.K. Harewood, Adult T cell leukemia-lymphoma (ATL): state of the art, Curr. Hematol. Malig. Rep. 13 (2018) 300–307, https://doi.org/10.1007/S11899-018-0458-6.
[9] K. Tsukasaki, A. Marçais, R. Nasr, K. Kato, T. Fukuda, O. Hermine, A. Bazarbachi, Diagnostic approaches and established treatments for adult T cell leukemia lymphoma, Front. Microbiol. 11 (2020), https://doi.org/10.3389/FMICB.2020.01207.
[10] M. Yamagishi, Y. Suzuki, T. Watanabe, K. Uchimaru, Clonal Selection and Evolution of HTLV-1-Infected Cells Driven by Genetic and Epigenetic Alteration. Viruses *14*, 2022, https://doi.org/10.3390/V14030587.
[11] N. Kawano, Y. Nagahiro, S. Yoshida, Y. Tahara, D. Himeji, T. Kuriyama, T. Tochigi, T. Nakaike, T. Shimokawa, K. Yamashita, et al., Clinical features and treatment outcomes of opportunistic infections among human T-lymphotrophic virus type 1 (HTLV-1) carriers and patients with adult T-cell leukemia-lymphoma (ATL) at a single institution from 2006 to 2016, J. Clin. Exp. Hematop. 59 (2019) 156–167, https://doi.org/10.3960/JSLRT.18032.

[12] A.F. Porto, F.A. Neva, H. Bittencourt, W. Lisboa, R. Thompson, L. Alcântara, E.M. Carvalho, HTLV-1 decreases Th2 type of immune response in patients with strongyloidiasis, Parasite Immunol. 23 (2001) 503–507, https://doi.org/10.1046/J.1365-3024.2001.00407.X.
[13] M. Montes, C. Sanchez, K. Verdonck, J.E. Lake, E. Gonzalez, G. Lopez, A. Terashima, T. Nolan, D.E. Lewis, E. Gotuzzo, et al., Regulatory T cell expansion in HTLV-1 and strongyloidiasis Co-infection is associated with reduced IL-5 responses to Strongyloides stercoralis antigen, PLoS Neglected Trop. Dis. 3 (2009), https://doi.org/10.1371/JOURNAL.PNTD.0000456.
[14] E.J. Stevens, K.A. Bates, K.C. King, Host microbiota can facilitate pathogen infection, PLoS Pathog. 17 (2021) e1009514, https://doi.org/10.1371/JOURNAL.PPAT.1009514.
[15] A.R. Al Anazi, Gastrointestinal opportunistic infections in human immunodeficiency virus disease, Saudi J. Gastroenterol. 15 (2009) 95, https://doi.org/10.4103/1319-3767.48965.
[16] A.S. Zevin, L. McKinnon, A. Burgener, N.R. Klatt, Microbial translocation and microbiome dsybiosis in HIV-associated immune activation, Curr. Opin. HIV AIDS 11 (2016) 182, https://doi.org/10.1097/COH.0000000000000234.
[17] M. Tag-Adeen, K. Hashiguchi, Y. Akazawa, K. Ohnita, S. Yasushi, N. Daisuke, K. Nakao, An unusual presentation of adult T-cell leukemia/lymphoma, Ecancermedicalscience 12 (2018), https://doi.org/10.3332/ECANCER.2018.801.
[18] Y. Nishimoto, S. Mizutani, T. Nakajima, F. Hosoda, H. Watanabe, Y. Saito, T. Shibata, S. Yachida, T. Yamada, High stability of faecal microbiome composition in guanidine thiocyanate solution at room temperature and robustness during colonoscopy, Gut 65 (2016) 1574–1575, https://doi.org/10.1136/GUTJNL-2016-311937.
[19] M. Iwanaga, T. Watanabe, A. Utsunomiya, A. Okayama, K. Uchimaru, K.R. Koh, M. Ogata, H. Kikuchi, Y. Sagara, K. Uozumi, et al., Human T-cell leukemia virus type I (HTLV-1) proviral load and disease progression in asymptomatic HTLV-1 carriers: a nationwide prospective study in Japan, Blood 116 (2010) 1211–1219, https://doi.org/10.1182/BLOOD-2009-12-257410.
[20] M. Shimoyama, Diagnostic criteria and classification of clinical subtypes of adult T-cell leukaemia-lymphoma, Br. J. Haematol. 79 (1991) 428–437, https://doi.org/10.1111/J.1365-2141.1991.TB08051.X.
[21] M. Arumugam, J. Raes, E. Pelletier, D. Le Paslier, T. Yamada, D.R. Mende, G.R. Fernandes, J. Tap, T. Bruls, J.M. Batto, et al., Enterotypes of the human gut microbiome, Nature 473 (2011) 174–180, https://doi.org/10.1038/nature09944.
[22] Kamihira, S., Atogami, S., Sohda, H., Momita, S., Yamada, Y., and Tomonaga, M. Significance of soluble interleukin-2 receptor levels for evaluation of the progression of adult T-cell Leukemia. 10.1002/1097-0142(19940601)73:11.
[23] H. Shiroma, Y. Darzi, E. Terajima, Z. Nakagawa, H. Tsuchikura, N. Tsukuda, Y. Moriya, S. Okuda, S. Goto, T. Yamada, Enteropathway: the metabolic pathway database for the human gut microbiota, bioRxiv 2023 (2023) 6, https://doi.org/10.1101/2023.06.28.546710, 28.546710.
[24] A.K. Niemi, C. Brown, T. Moore, G.M. Enns, T.M. Cowan, Evidence of redox imbalance in a patient with succinic semialdehyde dehydrogenase deficiency, Mol. Genet. Metab. Reports 1 (2014) 129, https://doi.org/10.1016/J.YMGMR.2014.02.005.
[25] J.D. Hayes, A.T. Dinkova-Kostova, K.D. Tew, Oxidative stress in cancer, Cancer Cell 38 (2020) 167–197, https://doi.org/10.1016/J.CCELL.2020.06.001.
[26] A. Gupta, A. Pande, A. Sabrin, S.S. Thapa, B.W. Gioe, A. Grove, MarR family transcription factors from Burkholderia species: hidden clues to control of virulence-associated genes, Microbiol. Mol. Biol. Rev. 83 (2019), https://doi.org/10.1128/MMBR.00039-18.
[27] V. Méndez, L. Agulló, M. González, M. Seeger, The homogentisate and homoprotocatechuate central pathways are involved in 3- and 4-hydroxyphenylacetate degradation by Burkholderia xenovorans LB400, PLoS One 6 (2011), https://doi.org/10.1371/JOURNAL.PONE.0017583.
[28] B. Galán, A. Kolb, J.M. Sanz, J.L. García, M.A. Prieto, Molecular determinants of the hpa regulatory system of Escherichia coli: the HpaR repressor, Nucleic Acids Res. 31 (2003) 6598, https://doi.org/10.1093/NAR/GKG851.
[29] J. Ramirez, F. Guarner, L. Bustos Fernandez, A. Maruy, V.L. Sdepanian, H. Cohen, Antibiotics as major disruptors of gut microbiota, Front. Cell. Infect. Microbiol. 10 (2020) 731, https://doi.org/10.3389/FCIMB.2020.572912/BIBTEX.
[30] A. Dykie, T. Wijesinghe, A.B. Rabson, K. Madugula, C. Farinas, S. Wilson, D. Abraham, P. Jain, Human T-cell leukemia virus type 1 and Strongyloides stercoralis: partners in pathogenesis, Pathogens 9 (2020) 1–22, https://doi.org/10.3390/PATHOGENS9110904.
[31] M. Satoh, H. Toma, K. Sugahara, K.I. Etoh, Y. Shiroma, S. Kiyuna, M. Takara, M. Matsuoka, K. Yamaguchi, K. Nakada, et al., Involvement of IL-2/IL-2R system activation by parasite antigen in polyclonal expansion of CD4+25+ HTLV-1-infected T-cells in human carriers of both HTLV-1 and S. stercoralis, Oncogene 2116 21 (2002) 2466–2475, https://doi.org/10.1038/sj.onc.1205329, 2002.
[32] M. Mahgoub, J.I. Yasunaga, S. Iwami, S. Nakaoka, Y. Koizumi, K. Shimura, M. Matsuoka, Sporadic on/off switching of HTLV-1 Tax expression is crucial to maintain the whole population of virus-induced leukemic cells, Proc. Natl. Acad. Sci. U. S. A 115 (2018) E1269–E1278, https://doi.org/10.1073/pnas.1715724115.
[33] M. Takahashi, M. Higuchi, G.N. Makokha, H. Matsuki, M. Yoshita, Y. Tanaka, M. Fujii, HTLV-1 Tax oncoprotein stimulates ROS production and apoptosis in T cells by interacting with USP10, Blood 122 (2013) 715–725, https://doi.org/10.1182/BLOOD-2013-03-493718.
[34] S. Chen, Y. Zhou, Y. Chen, J. Gu, fastp: an ultra-fast all-in-one FASTQ preprocessor, Bioinformatics 34 (2018) i884–i890, https://doi.org/10.1093/BIOINFORMATICS/BTY560.
[35] T. Rognes, T. Flouri, B. Nichols, C. Quince, F. Mahé, VSEARCH: a versatile open source tool for metagenomics, PeerJ 4 (2016), https://doi.org/10.7717/PEERJ.2584.
[36] W. Shen, S. Le, Y. Li, F. Hu, SeqKit: a cross-platform and ultrafast toolkit for FASTA/Q file manipulation, PLoS One 11 (2016) e0163962, https://doi.org/10.1371/JOURNAL.PONE.0163962.
[37] A. Amir, D. McDonald, J.A. Navas-Molina, E. Kopylova, J.T. Morton, Z. Zech Xu, E.P. Kightley, L.R. Thompson, E.R. Hyde, A. Gonzalez, et al., Deblur Rapidly Resolves Single-Nucleotide Community Sequence Patterns. mSystems, vol. 2, PDF, 2017, https://doi.org/10.1128/MSYSTEMS.00191-16/SUPPL_FILE/SYS002172091SF3.
[38] E. Kopylova, L. Noé, H. Touzet, SortMeRNA: fast and accurate filtering of ribosomal RNAs in metatranscriptomic data, Bioinformatics 28 (2012) 3211–3217, https://doi.org/10.1093/BIOINFORMATICS/BTS611.
[39] C. Camacho, G. Coulouris, V. Avagyan, N. Ma, J. Papadopoulos, K. Bealer, T.L. Madden, BLAST+: architecture and applications, BMC Bioinf. 10 (2009) 1–9, https://doi.org/10.1186/1471-2105-10-421/FIGURES/4.
[40] M. Martin, Cutadapt removes adapter sequences from high-throughput sequencing reads, EMBnet.journal 17 (2011) 10–12.
[41] B. Langmead, S.L. Salzberg, Fast gapped-read alignment with Bowtie 2, Nat. Methods 9 (2012) 357, https://doi.org/10.1038/NMETH.1923.
[42] D. Li, R. Luo, C.M. Liu, C.M. Leung, H.F. Ting, K. Sadakane, H. Yamashita, T.W. Lam, MEGAHIT v1.0: a fast and scalable metagenome assembler driven by advanced methodologies and community practices, Methods 102 (2016) 3–11, https://doi.org/10.1016/J.YMETH.2016.02.020.
[43] D. Hyatt, G.L. Chen, P.F. LoCascio, M.L. Land, F.W. Larimer, L.J. Hauser, Prodigal: prokaryotic gene recognition and translation initiation site identification, BMC Bioinf. 11 (2010) 1–11, https://doi.org/10.1186/1471-2105-11-119/TABLES/5.
[44] M. Steinegger, J. Söding, MMseqs2 enables sensitive protein sequence searching for the analysis of massive data sets, Nat. Biotechnol. 3511 35 (2017) 1026–1028, https://doi.org/10.1038/nbt.3988, 2017.
[45] B. Buchfink, K. Reuter, H.G. Drost, Sensitive protein alignments at tree-of-life scale using DIAMOND, Nat. Methods 184 18 (2021) 366–368, https://doi.org/10.1038/s41592-021-01101-x, 2021.
[46] K. Katoh, D.M. Standley, MAFFT multiple sequence alignment software version 7: improvements in performance and usability, Mol. Biol. Evol. 30 (2013) 772, https://doi.org/10.1093/MOLBEV/MST010.
[47] A. Stamatakis, RAxML version 8: a tool for phylogenetic analysis and post-analysis of large phylogenies, Bioinformatics 30 (2014) 1312, https://doi.org/10.1093/BIOINFORMATICS/BTU033.
[48] I. Letunic, P. Bork, Interactive Tree of Life (iTOL) v4: recent updates and new developments, Nucleic Acids Res. 47 (2019) W256–W259, https://doi.org/10.1093/NAR/GKZ239.

[49] D.H. Parks, M. Chuvochina, D.W. Waite, C. Rinke, A. Skarshewski, P.A. Chaumeil, P. Hugenholtz, A standardized bacterial taxonomy based on genome phylogeny substantially revises the tree of life, Nat. Biotechnol. 3610 36 (2018) 996–1004, https://doi.org/10.1038/nbt.4229, 2018.
[50] A.L. Mitchell, A. Almeida, M. Beracochea, M. Boland, J. Burgin, G. Cochrane, M.R. Crusoe, V. Kale, S.C. Potter, L.J. Richardson, et al., MGnify: the microbiome analysis resource in 2020, Nucleic Acids Res. 48 (2020) D570–D578, https://doi.org/10.1093/NAR/GKZ1035.
[51] M. Kanehisa, S. Goto, KEGG: Kyoto Encyclopedia of genes and genomes, Nucleic Acids Res. 28 (2000) 27, https://doi.org/10.1093/NAR/28.1.27.